Theoretical design and experimental study of magnetic circuit for magnetorheological (MR) damper of shear-valve mode

Yuxi Liu[1,*], Aihua Li[2], Zhangdong Sun[3], Song Chen[4]
[1]School of Smart Health, Chongqing College of Electronic Engineering, Chongqing, 401331, China
[2]Department of Gastroenterology, Chongqing University Cancer Hospital, Chongqing 400030, China
[3]Hubei University of Automotive Technology, Shiyan 442002, Hubei, China
[4]College of Mechanical Engineering, Chongqing University of Technology, Chongqing 400044, China

*Corresponding author: liugw215@126.com

ABSTRACT Based on the analysis of shear flow and differential pressure flow of Magnetorheological (MR) fluids, the damping force of MR shear-valve is analysed and calculated, and the magnetic circuit of MR damper is designed. Based on the designed magnetic circuit, the degree of magnetic saturation and the dynamic characteristics of MR fluid damper, such as impedance, current, velocity and frequency are investigated. The results of the magnetic induction test for damping clearance show that the magnetic induction intensity reaches 0.55Twhen the coil current is 1.4A. The bench test results show that when the piston speed is constant and the current is less than 1.36A, the variation of damping force increases significantly. Nevertheless, when the current is greater than 1.36A, the damping force tends to be stable and the coil reaches magnetic saturation. The energy indication characteristics of MR damper also show the same trend, which are consistent with the theoretical results. The results of this study can provide useful guidance for the magnetic circuit design of shear-valve MR fluid damper.

INDEX TERMS MR fluid, shear-valve mode, MR damper, magnetic circuit, energy indication characteristic

I. INTRODUCTION

WHEN the magnetic field is applied, iron particles in the MR fluid behave as dipoles and tend to align with the constant flux [1-3]. Based on this characteristic, magnetorheological fluids (MRF) are widely used in valve, clutch, brake, and damper systems [4-6].

According to the force state and flow pattern of MR fluids, MR damper could be classified into valve mode, shear mode, squeeze mode and any combinations of these three basic modes. In practice, many studies have been carried out with the valve mode [7], shear mode [8-10] and squeeze mode [11-12] or a combination of them [13]. In valve mode, the performance of MR damper control is negatively affected if the magnitude of excitations is small. In shear mode, the damping force generated from the MR effect is relatively small compared to other modes. In squeeze mode, the damper can achieve a high damping force, although it can only work effectively in a small vibration area [14].

Many researchers have demonstrated that the combined MRF modes can generate better performance than a single mode. For example, Eshgarf et al. compared and analyzed the properties and applications of MR fluid damper, valve and brake [15]. Wahed and Mcewan [16] combined the squeeze mode with shear-flow mode for a large damping force. Combined the shear mode with squeeze mode, Yazid et al. [17] designed MR damper. Currently, most research is focusing on a single mode or the combination of squeeze mode and shear mode. The research on the shear-valve mode MR damper is rare, and that on the mixed mode magnetic circuit design is even less. To this end, it is necessary to systematically investigate the magnetic circuit design of the combined shear-valve mode MR damper.

Magnetic circuit design is a critical part of MR damper, and its performance is directly affected by the structure and design parameters. Here the damping force produced by shear-valve MR damper is analyzed theoretically. Then, the magnetic circuit of MR damper is designed and its dynamic characteristics are tested experimentally. The obtained test results show the correctness of the theoretical design.

II. MR DAMPING FORCE ANALYSIS

The constitutive relation of Newtonian fluids is defined without magnetic field. When there is such a field, MR fluid has a certain yield stress, and is similar to that of a solid, whose constitutive relation is described by Bingham model [18].

$$\begin{cases} \tau = \tau_y(H)\,\mathrm{sgn}(\gamma) + \eta_0\gamma & \tau \geq \tau_y(H) \\ \dot{\gamma} = 0 & \tau < \tau_y(H) \end{cases} \quad (1)$$

where τ is the shear stress on MR field; η_0 is the viscosity of fluid without magnetic field; $\dot{\gamma}$ is the shear strain rate; $\tau_y(H)$ is the dynamic yield stress that changes with the magnetic field intensity H; and sgn(·)is the sign function.

Shear-valve mode dampers have two flow forms. One is that the piston squeezes the MR fluid by creating a pressure difference between the side chambers of the damper. This pressure difference forces the MR fluid to flow through the piston holes, and it is called pressure difference flow. The other one is the relative motion between the cylinder and the piston, which drags the MR fluid from one chamber to another through the radial clearance between the cylinder and the piston and is called shear flow. As a result, the total damping force of shear-valve MR dampers is a sum of the forces generated by the pressure difference flow F_p and the shear flow F_s.

A. VALVE MODE

In valve mode, the total damping force is the sum of the viscous ΔF_r and the magnetic field dependent force ΔF_{mr}. The damping force of the valve mode can be approximately expressed as [18]:

$$F_p(t) = \Delta P_r + \Delta P_{mr} = \frac{12\eta LQ}{wg^3} + \frac{f\tau_{mr}L}{g} \quad (2)$$

where η is the dynamic viscosity (Pa·s); Q is the flow rate (m^3 s); L, w and g are the length, width and clearance size respectively (m); τ_{mr} is the yield stress in response to the applied magnetic field (N/mm^2); f is an empirical factor that depends upon the specific value of ΔF_r and ΔF_{mr}, defined as:

f=2, When $\Delta F_{mr}/\Delta F_r < 1$;

f=3, When $\Delta F_{mr}/\Delta F_r \sim 1$.

Eq. (2) can be used for the design of MR fluid valve mode. The minimum volume of active fluid can be established as:

$$V = L \cdot w \cdot g = \frac{\eta}{\tau^2} \cdot \frac{F_r}{F_{mr}} \cdot F_{mr} \cdot S \quad (3)$$

This minimum volume is required to achieve a desired MR effect at a given flow rate Q with a specified pressure difference, the effective parameters are the diameter of the damping holes d and damping clearance length L.

B. SHEAR MODE

The total shear force can be separated into viscous F_r and the magnetic field dependent force F_{mr} in the shear mode. The force of shear mode can be approximately expressed as

$$F_s = F_r + F_{mr} = \tau_{mr} \cdot A + \frac{\eta \cdot S \cdot A}{g} \quad (4)$$

where S is a relative speed (m/s), and $A = Lw$.

Eq. (4) can be used for the design of MR fluid shear mode, and the minimum effective volume can be established as

$$V = L \cdot w \cdot g = \frac{\eta}{\tau^2} \cdot \frac{F_r}{F_{mr}} \cdot F_{mr} \cdot S \quad (5)$$

The total damping force should be a combination of Eq. (2) and Eq. (4) for shear-valve mode MR damper.

III. DESIGN AND ANALYSIS OF MAGNETIC CIRCUIT

A. MAGNETIC CIRCUIT DESIGN AND MAGNETIC INDUCTION CALCULATION

1) MAGNETIC CIRCUIT DESIGN

The shear-valve damper uses the reciprocating linear motion of the piston in its cylinder to squeeze MR fluids and force it to flow through the clearance and the damping hole between the cylinder and piston, generating a certain degree of damping force to realize vibration damping. The purpose of magnetic circuit design is to determine the ampere-turns of the coil, to ensure the maximum magnetic induction in working clearance and the largest MR damper in the controllable damping force. In addition, it should be also ensured that the coil temperature does not exceed permissible value and the coil size matches the piston size.

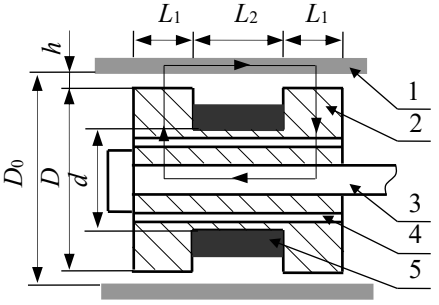

FIGURE 1. Configuration of the magnetic circuit of MR damper (1-Cylinder; 2-Piston; 3-Rod; 4-Damping hole; 5-Coil)

According to the experimental results, the magnetic circuit of the MR damper can be depicted as Figure 1.h is the radial clearance; D is the diameter of piston; D_0 is the inner diameter of the cylinder; $(2L_1+L_2)$ is the axial length of magnetic core, and d_0 is the diameter of damping holes.

It can be seen from Figure 1 that MR fluid is forced to flow through the piston hole due to the pressure difference between the chambers on both sides, as shown Figure 2(a). On the other hand, the MR fluids are sheared in the damping clearance when the piston reciprocates in the cylinder, as shown in Figure 2(b).

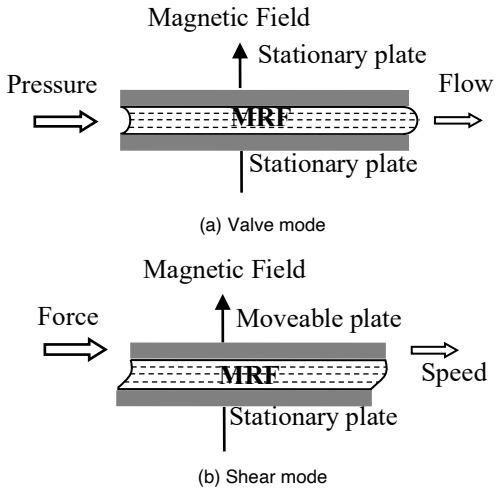

FIGURE 2. MRF operational modes. (a) Valve mode, (b) shear mode

2) MAGNETIC INDUCTION CALCULATION

According to the configuration of magnetic circuit, the region covered by magnetic lines can be divided into eight areas. Since the configuration is symmetrical, it is applied to the other half of the cylinder. The notation used for the damper size is shown in Figure 3.

DT4 is selected as the magnetic core material of areas 1, 2, 3, 4 and 5, and its saturation magnetization is 1.65T. The material of cylinder areas 6, 7, 8 is 45 steel and its saturation magnetization is 1.5T. MR fluids (MRF-J01) was developed by Chongqing Materials Research Institute, and the magnetic induction (B_{MRF}) of its saturation magnetization is 0.52T. Assuming the initial magnetic induction in the damping clearance is 0.52T, the magnetic induction intensity at the cross section of each region can be calculated based on the principal of magnetic flux.

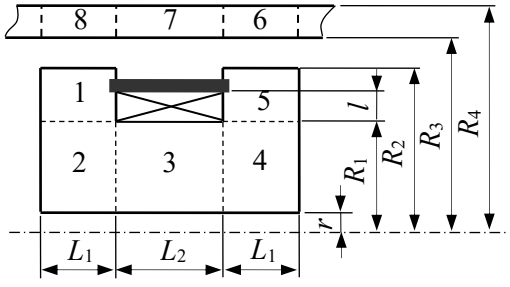

FIGURE 3. Area division of magnetic circuit

The magnetic field covers the whole area. According to the relative dimensions in Figure 3, the magnetic flux in the damping clearance can be determined by

$$\phi = B_{\mathrm{MRF}} S_{\mathrm{MRF}} \tag{6}$$

According to the value of the magnetic flux at each region, the magnetic induction of each region can be determined as shown in Table I.

TABLE I. Magnetic induction of each region(Units: T)

B1	B2	B3	B4	B5	B6	B7	B8
0.764	1.152	0.838	1.152	0.764	0.454	0.726	0.454

As shown in Table I, as the current in excitation coil increases, the MR fluid reaches magnetic saturation before magnetic saturation occurs in the rest areas of the damper. Thus, the damping force of the MR damper is adjustable before the MR fluid reaches magnetic saturation.

B. DETERMINING PARAMETERS OF SOLENOID

1) ELECTROMAGNETIC WIRE SELECTION

According to the principle of magnetic circuit design, under different working conditions, the allowable range of current density J can be determined as:

(1) Long-term working condition: J =2- 4A/mm^2;

(2) Repeated and short-time working condition: J=5-12A/mm^2;

(3) Short-time working condition: J =13-30A/mm^2.

Due to the rapid change of loading conditions in MR damper, the current density is selected as J= 10A/mm^2.

Assuming that the maximum current through the solenoid is I_{max}=3A, the wire diameter can be calculated as:

$$d_0 = 2 \times (I_{\max} / (\pi \times J))^{0.5} \tag{7}$$

where d_0=0.618mm.

According to the calculation, the wire specification of d_0=0.64mm and J=9.33A/mm^2 that complies with requirements of current density (GB6109.3-2008) are selected. The main parameters of the wire are shown in Table II.

TABLE II. Parameters of wire

Name	Type	Nominal diameter /mm	Out diameter /mm	Breakdown Voltage/V
Enameled copper wire	GB6109.3-2008	0.64	0.70	1 400

2) DETERMINATION AMPERE-TURNS OF COIL

According to the ampere circuit law, the total magnetic potential difference can be expressed as $\sum U = N \times I$, where N is the ampere- turns and I is the operating current in coil. $\sum U$ is also equal to the magnetic potential of magnetic circuit, and $\sum U = H_i \times l_i$, where U is the magnetic potential difference; H_i is the magnetic field intensity that can be obtained from the B-H curve of different material, and l_i is length of each area. Figure 4 and Figure 5 show the B-H curves for 45 steel and electrical iron DT4, respectively.

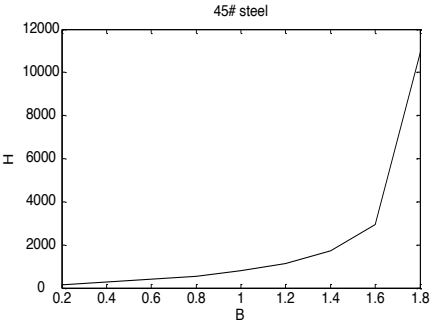

FIGURE 4. 45 Steel B-H curve

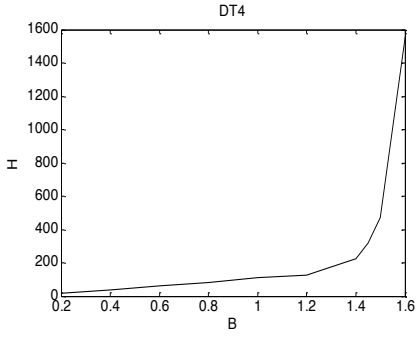

FIGURE 5. DT4 B-H curve

As shown in Table I, Figure 4 and Figure 5, the magnetic field intensity of each area can be obtained as shown in Table III.

TABLE III. Magnetic field intensity of each area (Units: A/m)

H1	H2	H3	H4	H5	H6	H7	H8
81	129	89	129	81	278	495	278

According to the experimental parameters of MRF (MRF-J01, Chongqing Materials Research Institute), the magnetic field intensity is 126 546.7A/m under the magnetic induction of B=0.52T. Since the width of the damping clearance is 1.5mm, the magnetic potential difference of MRF in working areas is F_{MRF}=189.8A.

According to Kirchhoff's second law of magnetic circuit, the total magnetic potential difference of each segment can be obtained as:

$$F' = \sum H_i l_i \qquad i = 1,2,3,\cdots 8 \tag{8}$$

Substituting the dimensions in Figure 3 and the magnetic field intensity of Table III into Eq.(8), it can be known that the magnetic potential difference is 25.73A. Since the damping clearance has two segments, the total magnetic potential difference is

$$\sum F = 2 \times F_{MRF} + F' \tag{9}$$

According to wire parameters in Table II, when the max current is 3A, the ampere-turns N =136 can be calculated by $\sum U = N \times I$. The effect of air leakage flux is neglected. The high-strength enameled wire of 0.70mm diameter is selected for the coil. To keep the current below its limit value, the ampere-turns $N$is selected as 300, where the current I =1.36A. That is, when the current reaches 1.36A, the magnetic induction reaches magnetic saturation in the damping clearance.

IV. EXPERIMENTAL RESULTS AND ANALYSIS

A special suspension test apparatus (MTS) is set up to investigate the damping force response of the MR damper at different currents. The reference standard for this MR damper bench test is QC/T545-1999 Bench Test Method for Automobile Barrel Shock Absorbers. In addition, the effectiveness of damper design can be further verified by comparing the results of experimental tests and theoretical model calculation. A schematic diagram of the test apparatus is shown in Figure 6.

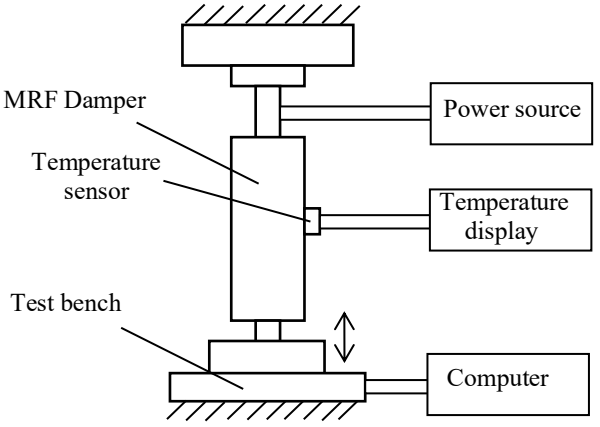

FIGURE 6. The schematic diagram of the test apparatus of MR damper

A. MAGNETIC INDUCTION TESTING IN DAMPING CLEARANCE

The coil is energized with stabilized voltage supply, and a digital readout Teslameter is used to measure the magnetic induction in a damping clearance. Whenever the current is altered, the average magnetic induction in the damping clearance can be determined by

$$B_a = (B_{\max} + B_{\min}) / 2 \tag{10}$$

where $B_{\max}$ and $B_{\min}$ are the maximum and minimum magnetic induction in the damping clearance respectively.

The average magnetic induction in the damping clearance changes with the coil current. The relationship of magnetic induction and coil current is shown in Figure 7. The magnetic induction of the damping clearance changes significantly when the coil current varies from 0.2A to 1.8A. The magnetic induction reaches 0.55T when the coil current is 1.4A, which is consistent with the results obtained from theoretical calculation. In practice, the MRF in the damper clearance will first reach magnetic saturation. In addition,

the larger damping force will be obtained when the current is minimum, which helps to keep the heat generated by the coil to a minimum.

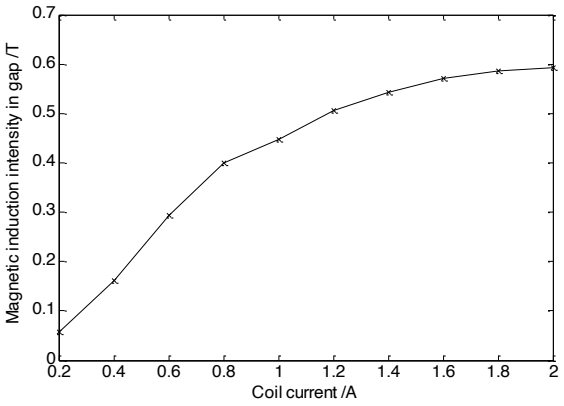

FIGURE 7. The relationship between magnetic induction and current

B. EFFECTS OF CURRENT ON DAMPING FORCE

The load in this experiment is composed of sine wave excitation with a frequency of 1Hz, and the displacement of the piston is ±40mm. The relationship between the damping force and the current is obtained by adjusting the intensity of the input current, and the test results as shown in Figure 8. The test results show that when the piston velocity is constant, the current remains below 1.36A. The magnitude and range adjustment of damping force significantly increase. When the currents are larger than 1.36 A, not only the damping force tends to stabilize, but also the damper´s adjustability tends to decline due to magnetic saturation, which is consistent with the theoretical results.

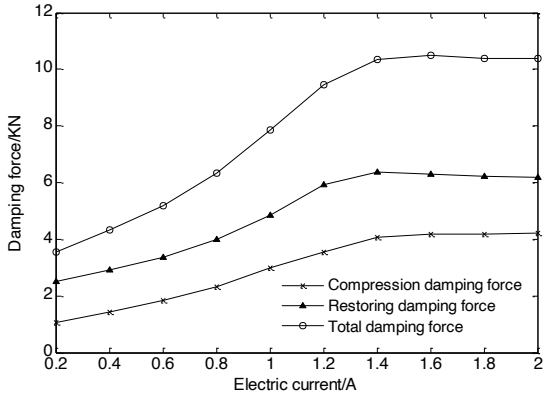

FIGURE 8. Relationship between damping force and current

C. ENERGY INDICATION CHARACTERISTIC OF MR DAMPER

When the load conditions are the same, the characteristic curve of damping force-displacement is obtained by adjusting the current in 0.2A increments from 0 to 1.8A, the current increases gradually along the arrow (Figure 9).

It can be seen from Figure 9 that the area within the curve increases with the increase of current, which means that the energy consumption of each vibration cycle also increases. This demonstrates the controllability of the MR damper and the relationships between the current and the damper force. Furthermore, as the current increases, the magnitude of the damping force increases rapidly at first. When the current is larger than 1.4A, the increase magnitude of damping force is small.

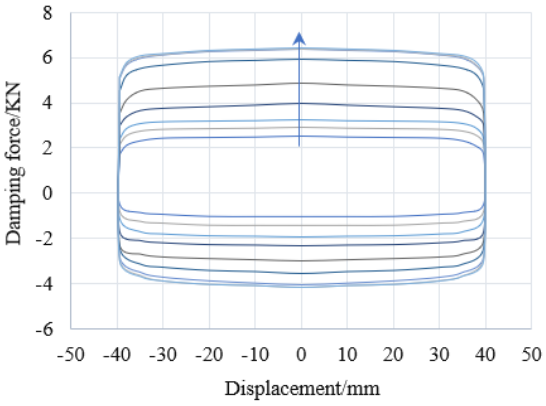

FIGURE 9. Characteristic curves of damping force – displacement

When the current is 1.4A, 1.6A and 1.8A, respectively, the curves almost superimpose each other, and the magnitude of the damping force changes little. When the magnetic induction increases to a certain extent, the magnetic permeability of the material will decrease with the increase of the magnetic field intensity, which means that the material reaches magnetic saturation. Due to the magnetic saturation characteristics of excitation materials, the increase of magnetic induction is quite small when the current reaches a certain value, indicating that the same case will occur to the magnitude of the MR damping force.

V. CONCLUSIONS

(1) Magnetic induction intensity in damping clearance is controlled by the excitation current of the coil, and the damping force can also be controlled by adjusting the current.

(2) The increase of the coil current first leads to the magnetic saturation of MR fluid in the damping clearance, then the damping force reaches the maximum value at low current.

(3) The damping force tends to be stable when the current is greater than 1.36A, which shows that MRF in damping clearance reaches magnetic saturation, and the reliability of the magnetic circuit design is verified by the tests carried out.

(4) The bench test results shown that the damping force increases rapidly with the increase of the current, and the increase of damping force is small when the current exceeds

a certain value, and indicates the rationality of the damper design.

ACKNOWLEDGEMENT

This work was supported by the Science and Technology Research Program of Chongqing Municipal Education Commission (Grant No. KJQN202203110), Chongqing Scientific Research Institute Performance Incentive guidance special project (Grant No.cstc2020jxjl130017), and Natural Science Foundation of Chongqing (cstc2020jcyj-msxmX0402).

REFERENCES

[1] R. Asiaban, H. Khajehsaeid, E. Ghobadi, M. Jabbarid, "New magneto-rheological fluids with high stability: Experimental study and constitutive modeling," *Polymer Testing*, vol. 87, pp. 106512, 2020. https://doi.org/10.1016/j.polymertesting.2020.106512

[2] P. Pei, Y. Peng, "Constitutive modeling of magnetorheological fluids: A review," *Journal of Magnetism and Magnetic Materials*, vol. 550, pp. 169076, 2022. https://doi.org/10.1016/j.jmmm.2022.169076

[3] M. Kumar, A. Kumar, R. K. Bharti, H. N. S. Yadav, M. Das, "A review on rheological properties of magnetorheological fluid for engineering components polishing," *Materials Today: Proceedings*, vol. 56, no. Part 3, pp. A6-A12, 2022. *https://doi.org/10.1016/j.matpr.2021.11.611*

[4] L. Prabhu, S.S. Kumar, D. Dinakaran, R. Jawahar, "Improvement of chatter stability in boring operations with semi active magneto-rheological fluid damper," *Materials Today: Proceedings*, vol. 33, no. Part 1, pp. 420-427, 2020. https://doi.org/10.1016/j.matpr.2020.04.651

[5] Y. Liu, Y. Zhang, B. Tang, M. Gao, J. Dai, "Introducing the thermal field into multi-physics coupling for the modeling of MR fluid-based micro-brake," *International Journal of Heat and Mass Transfer*, vol. 180, pp. 121785, 2021. https://doi.org/10.1016/j.ijheatmasstransfer.2021.121785

[6] J. Yu, X. Dong, X. Su, S. Qi, "Development and characterization of a novel rotary magnetorheological fluid damper with variable damping and stiffness," *Mechanical Systems and Signal Processing*, vol. 165, pp. 108320, 2022. https://doi.org/10.1016/j.ymssp.2021.108320

[7] J.S. Kumar, D.G. Alex, P.P. Sam, "Synthesis of Magnetorheological fluid Compositions for Valve Mode Operation," *Materials Today: Proceedings*, vol. 22, no. Part 4, pp. 1870-1877, 2020. https://doi.org/10.1016/j.matpr.2020.03.086

[8] A. Dargahi, R. Sedaghati, S. Rakheja, "On the properties of magnetorheological elastomers in shear mode: Design, fabrication and characterization," *Composites Part B: Engineering*, vol. 159, pp. 269-283, 2019. https://doi.org/10.1016/j.compositesb.2018.09.080

[9] X. Liu, D.Ye, X. Gao, F. Li, M. Sun, H. Zhang, T. Tu, H. Yu, "Normal force for static and steady shear mode in magnetorheological fluid," *Journal of Magnetism and Magnetic Materials*, vol. 398, pp. 137-140, 2016. https://doi.org/10.1016/j.jmmm.2015.09.009

[10] J. Huang, X. Chen, L. Zhong, "Analysis and Testing of MR Shear Transmission Driven by SMA Spring," *Advances in Materials Science and Engineering*, vol. 2013, pp. 307207, 2013. https://doi.org/10.1155/2013/307207

[11] Z. Liu, F. Li, X. Li, J. Xu, "Characteristic analysis and squeezing force mathematical model for magnetorheological fluid in squeeze mode," *Journal of Magnetism and Magnetic Materials*, vol. 529, pp. 167736, 2021. https://doi.org/10.1016/j.jmmm.2021.167736

[12] A. Erenchunac, B. Blanco, N. Gil-Negrete, B. Wang, L. Kari, "Effect of lubrication on the mechanical behavior of magnetorheological elastomers in compression mode," *Polymer Testing*, vol. 111, pp. 107617, 2022. https://doi.org/10.1016/j.polymertesting.2022.107617

[13] G. Hu, L. Wu, Y. Deng, L. Yu, G. Li, "Optimal design and performance analysis of magnetorheological damper based on multiphysics coupling model," *Journal of Magnetism and Magnetic Materials*, vol. 558, pp. 169527, 2022. https://doi.org/10.1016/j.jmmm.2022.169527

[14] H. Vatandoost, M. Hemmatian, R. Sedaghati, S. Rakheja, "Dynamic characterization of isotropic and anisotropic magnetorheological elastomers in the oscillatory squeeze mode superimposed on large static pre-strain," *Composites Part B: Engineering*, vol. 182, pp. 107648, 2020. https://doi.org/10.1016/j.compositesb.2019.107648

[15] H. Eshgarf, A.A. Nadooshan, A. Raisi, "An overview on properties and applications of magnetorheological fluids: Dampers, batteries, valves and brakes," *Journal of Energy Storage*, vol. 50, pp. 104648, 2022. https://doi.org/10.1016/j.est.2022.104648

[16] A.K. EiWahed, C.A. Mcewan, "Design and performance evaluation of magnetorheological fluids under single and mixed modes," *Journal of Intelligent Material Systems and Structures*, vol. 22, no. 7, pp. 631-643, 2011. https://doi.org/10.1177/1045389X11404453

[17] I. I. M. Yazid, S. A. Mazlan, T. Kikuchi, H. Zamzuri, F. Imaduddin, "Design magnetorheological damper with a combination of shear and squeeze modes," *Materials and Design*, vol. 54, pp. 87-95, 2014. https://doi.org/10.1016/j.matdes.2013.07.090

[18] Z. Parlak, T. E. Call, "Optimal design of MR damper via finite element analyses of fluid dynamic and magnetic field," *Mechatronics*, vol. 22, no. 6, pp. 890-903, 2012. https://doi.org/10.1016/j.mechatronics.2012.05.007